Archives of Razi Institute, Vol. 75, No. 4 (2020) 427-437

DOI: 10.22092/ari.2019.127251.1377

Original Article

Identification of Conformational B-cell Epitopes in Diphtheria Toxin at Varying Temperatures Using Molecular Dynamics Simulations

Ghaderi, S. [1], Bozorgmehr, M. R. [2], Ahmadi, M. [3*], Tarahomjoo, Sh. [4]

1. Division of Central Laboratory, Department of Biotechnology, Razi Vaccine and Serum Research Institute, Agricultural Research, Education and Extension Organization (AREEO), Karaj, Iran
2. Department of Chemistry, Mashhad Branch, Islamic Azad University, Mashhad, Iran
3. Razi Vaccine and Serum Research Institute, Agricultural Research, Education and Extension Organization (AREEO), Karaj, Iran
4. Division of Genomics and Genetic Engineering, Department of Biotechnology, Razi Vaccine and Serum Research Institute, Agricultural Research, Education and Extension Organization (AREEO), Karaj, Iran

Received 29 July 2019; Accepted 15 September 2019
Corresponding Author: m.ahmadi1981@gmail.com

Abstract

The changes in temperature levels can potentially affect the toxins in terms of stability and immunological properties via alteration of their structures. Diphtheria Toxin (DT) is highly considered by scientists since its mechanism of action is similar to those of most bacterial toxins, such as botulinum, tetanus, and anthrax. The protection of conformational B-cell epitopes is critically important in the process of diphtheria vaccine production. This study aimed to evaluate the conformational changes of the DT structure at three different temperature levels (27˚C, 37˚C, and 47˚C) using molecular dynamic simulations. Secondary structures were analyzed in YASARA software. According to the results, significant decreases were observed in percentages of the β-sheets, turns, and the helices of the DT structure at 47˚C in comparison with those at 27˚C and 37˚C. Furthermore, the tertiary structure of the DT was compared at different temperatures using the contact map. Accordingly, the results showed that the root-mean-square deviation of the DT structure increased upon temperature rising. In addition, amino acids D68, G128, G171, C186, and K534-S535 at 27˚C and 37˚C, as well as amino acids G26, P38, S291, T267, H384, A356, and V518 at 47˚C showed higher root mean square fluctuation values. The finding demonstrated that the stability of the DT structure decreased at high temperature (47˚C). The solvent-accessible surface area diagram showed that the hydrophobicity of the DT structure increased via temperature rising, and the amino acid residues belonging to B-cell epitopes extended through increasing temperature. However, B-cell epitopes belonging to the junction region of chains A and B were only present at 37˚C. The results of this study are expected to be applicable for determining a suitable temperature level for the production process of the diphtheria vaccine.

Keywords: B-cell epitope, Diphtheria toxin, Molecular dynamics simulation, Stability, Temperature

Identification des épitopes Conformationnels des Lymphocytes B dans la Toxine Diphtérique à des Températures Variables en Utilisant des Simulations de Dynamique Moléculaire

Résumé: Les changements de niveaux de température peuvent potentiellement affecter les toxines en termes de stabilité et de propriétés immunologiques via l'altération de leurs structures. La toxine diphtérique (TD) est très étudiée par les scientifiques car son mécanisme d'action est similaire à ceux de la plupart des toxines bactériennes, telles que le botulisme, le tétanos et l'anthracis. La protection des épitopes conformationnels des lymphocytes B est d'une importance cruciale dans le processus de production du vaccin antidiphtérique. Cette

étude visait à évaluer les changements conformationnels de la structure de la TD à trois température différentes (27˚C, 37˚C et 47˚C) à l'aide de simulations de dynamique moléculaire. Les structures secondaires ont été analysées dans le logiciel YASARA. Selon les résultats, des diminutions significatives ont été observées dans les pourcentages des feuillets β, des spires et des hélices de la structure de la TD à 47°C par rapport à ceux observés à 27°C et 37°C. De plus, la structure tertiaire de la TD a été comparée à différentes températures en utilisant la carte de contact. Les résultats de cette étude ont montré que la déviation quadratique moyenne de la structure de la TD augmentait lors de l'augmentation de la température. En outre, les acides aminés D68, G128, G171, C186 et K534-S535 à 27°C et 37°C, ainsi que les acides aminés G26, P38, S291, T267, H384, A356 et V518 à 47°C ont montré des valeurs de fluctuation quadratique moyenne plus élevées. Ces résultats ont révélé que la stabilité de la structure de la TD diminuait à haute température (47°C). Le diagramme de surface accessible aux solvants a montré que l'hydrophobicité de la structure de la TD augmentait suite à l'augmentation de température, et les résidus d'acides aminés appartenant aux épitopes de lymphocytes B se prolongeaient. Cependant, les épitopes des cellules B appartenant à la région de jonction des chaînes A et B n'étaient présents qu'à 37°C. Les résultats de cette étude devraient être applicables pour déterminer un niveau de température approprié pour le processus de production d'un vaccin contre la diphtérie.

Mots-clés: Epitopes de cellules B, Toxine diphtérique, Simulation de dynamique moléculaire, Stabilité, Température

Introduction

Diphtheria Toxin (DT) is a protein of 535 residues that is composed of three structural domains with almost equal sizes, including catalytic (C) (1-193), transmembrane (T) (201-378), and receptor binding (R) domains (386-535) (Chenal et al., 2002). The T and R domains are connected by a hinge loop (379-386); however, disulfide bonds C to T domains (C186-C201) (Chenal et al., 2002). Moreover, the C domain is found in A fragment, whereas T and R domains are located in the B fragment (Menestrina et al., 1994).

A fragment of the toxin can be released from the whole toxin by proteolysis and reduction of the disulfide bond between A and B chains. In isolated form, the A fragment can catalyze ADP ribosylation (Gordon and Leppla, 1994). It has been observed in some experimental studies that high temperatures may make changes in the DT conformation, and these changes were considered the cause of denaturation. The in vitro experimental methods have put forward that the thermal transition is irreversible at a level ranges from 48˚C to 51˚C (Zhao and London, 1986).

Previous studies suggest that the effect of high temperature on toxin is to destroy the interactions stabilizing the native conformation and structure of DT (Guerineau et al., 2003). It has been hypothesized that the tertiary structure of DT, which is crucial for its translocation through cell membranes, is strongly influenced by pH, temperature, and the hydrophobic environment (London, 1992; Oh et al., 1996; Ghaderi et al., 2016). Although the findings of previous experimental studies strongly support this hypothesis, the lack of a computational investigation is seriously felt in this case.

In this study, different temperatures were compared in terms of MD simulation results of the DT structure since it was aimed to investigate the influence of temperature on its conformational stability. These results were compared with measures, including the RMSF, Rg, RMSD, and SASA. The secondary structures were also analyzed at different temperatures (i.e., 27˚C, 37˚C, and 47˚C). The tertiary structures were then compared using contact maps. In the second part of the present study, the effect of temperature was investigated on the DT's B-cell epitopes.

Material and Methods

This study evaluated the crystal structure of wild type DT from PDB entry 1F0L. This structure has been determined by X-ray diffraction at 1.55 Å resolution and pH 6.5 (Steere and Eisenberg, 2000). The

YASARA view (Krieger and Vriend, 2015), which is one of the most robust, stable, and widely used programs of molecular visualization, was used to preview the DT structure. The protonation state (i.e., the addition of missing protons to atoms) of the structure was set to neutral pH for each of the three temperature levels, including 27˚C, 37˚C, and 47˚C by H++ webserver (Anandakrishnan et al., 2012). The MD simulations were performed by GROMACS 4.5.4 package (Abraham et al., 2015) in which AMBER99SB (Salomon-Ferrer et al., 2013) was selected due to its desirable efficiency in protein simulation as the force field (Hornak et al., 2006). Periodic boundary conditions were also utilized in this study (Satpathy et al., 2010).

Moreover, three 9.5×9.5×9.5 (nm^3) simulation boxes were defined for the DT protein, and then TIP3P water was added to them (Jorgensen et al., 1983). The reason for selecting a cubic shape for the simulation box was its simplicity and high frequency of usage by researchers. To neutralize the system, the appropriate numbers of Na^+ and Cl^- ions were added to each box. Furthermore, to eliminate any undesirable contact atoms and initial kinetic energy in the simulation boxes, the energy was minimized by applying the steepest descent algorithm (Arfken, 1985). Subsequently, each of the defined systems reached equilibrium in two ensembles of NVT and NPT (at a fixed pressure of 1 bar) simulations. For both stages of the ensembles, a V-rescale algorithm was employed as the coupling time (Johnson et al., 2012). In total, three different levels of 27˚C, 37˚C, and 47˚C were considered temperature parameters for the above-mentioned simulations boxes. Furthermore, a velocity-rescaling thermostat was used to prolong a constant temperature (Bussi et al., 2007). The Parrinello-Rahman barostat was employed in any equilibration steps and MD simulations to maintain pressure at the selected set level during simulations (Parrinello et al., 1983).

For each component of the systems, the Particle Mesh Ewald algorithm was used to calculate the electrostatic interactions (Darden et al., 1993). Furthermore, to fix the chemical bonds formed between protein molecules, the Linear Constraint Solver algorithm was used in this study (Hess et al., 1997). All bonds containing hydrogens were constrained using the SHAKE algorithm (Kräutler et al., 2001). Once the forces acting on each of the system atoms were calculated, the positions of these atoms were moved according to Newton's laws of motion, which was integrated into the system by the Verlet algorithm (Grubmüller et al., 1991). A total of three MD simulations were performed at 50 ns. The assignment of secondary structures was performed using Kabsch and Sander (1983) as well as YASARA software, whereas three dimensional (3D) structures were computed and analyzed using CMView (version 1.1.1) which is an interactive contact map visualization tool (Vehlow et al., 2011). To predict the discontinuous B-cell epitopes of DT, ElliPro was utilized which is a structure-based tool to predict the conformational epitopes (http://tools.iedb.org/ellipro/). All simulations were repeated to assess the test-retest reliability of the results.

Results

The RMSF of all DT's residues was calculated during 50 ns MD simulations conducted at three different temperature levels, including 27˚C, 37˚C, and 47˚C. The RMSF is a metric measuring the average atomic mobility of atoms, especially those located on the backbone (N, Cα, and C atoms) (Vendome et al., 2011). The amino acid residues, including D68, G128, G171, C186-C201, and K534-S535 showed the highest fluctuations in the DT structure at 27˚C (Figure 1). The most unstable amino acids at 37˚C were D68, K125, G171, C186, and K534. However, the fluctuation of C186 at 37˚C was much higher than that at two other temperatures in the region including the disulfide bind of fragments A and B (C186-C201). The most fluctuating residues at 47˚C were G26, P38, S291,

T267, H384, A356, and V518. Furthermore, the larger values of RMSF indicate significant increases in random motions, instability of the residues, and flexibility of key regions of proteins (Zhao et al., 2015). The interaction of a protein with a ligand and its biological partners is critically influenced by the conformational flexibility (Purohit and Sethumadhavan, 2009; Purohit et al., 2011; Rajendran et al., 2012). The comparison of our results at 37˚C with those at 27˚C and 47˚C indicated that the largest fluctuations were observed in R and C domains (Figure 1).

The amino acid residues K534-S535 showed the highest flexibility at 27˚C, whereas at 37˚C, the amino acids C186-C201 obtained the highest flexibility. Furthermore, our results indicated that residues located in fragment B were more flexible at 47˚C. This disulfide bridge (C186-C201) is crucial for toxin activity, and its reduction following cleavage of the loop results in the separation of the C from T and R domains, as well as a loss of toxicity (Chenal et al., 2002). This region linking C to T domains is on the trans side of the membrane while disulfide bonds introduced inside the C domain block translocation (Falnes and Olsnes, 1995). Attempts to produce synthetic or recombinant vaccines from fragments of DT have been described in this study.

The synthetic peptide (residues 188-201 of DT corresponding to the loop connecting the C domain to the T domain) elicited protection against DT in guinea pigs (Audibert et al., 1981; Boquet et al., 1982). Therefore, it is critical to conserving the epitopes of this region in vaccine development.

The Rg is a parameter that indicates the equilibrium conformation of a total system determining the protein structure compactness (Lobanov et al., 2008). The compactness is obtained by dividing the accessible surface area of a protein by that of the ideal sphere of the same volume (Lobanov et al., 2008). Figure 2 illustrates the Rg values of DT structures at 27˚C, 37˚C, and 47˚C during MD simulations, indicating that the DT structure had the highest compactness (i.e. the minimum Rg) at 27˚C and 37˚C.

A standard measure for comparison of two structures can be a rigid body translation and rotation of one structure concerning the other by a least-squares superposition procedure (Diamond, 1976; Kabsch, 1976; Diamond, 1988). Following that, the difference between the two structures might be computed via the root-mean-square deviation (RMSD) of the Cartesian positions of the corresponding atoms (Brüschweiler, 2003). This metric is also frequently used in NMR spectroscopy to evaluate the mutual similarity of the lowest energy structures in an ensemble derived from the refinement process (Laurents et al., 2001; Kövér et al., 2008; Zhou et al., 2008).

The profile of the RMSD of DT at different temperature levels obtained via MD simulation was given in Figure 3. The RMSD value of DT at 27˚C (RMSD=0.1082 nm) was similar to that at 37˚C (RMSD=0.1471 nm). However, the highest RMSD value was observed at 47˚C (RMSD=1.3699 nm). This result suggested that the conformational stability of the DT structure at 27˚C was similar to that at 37˚C and much better than that at 47˚C. Conformational stability of DT has a critical role in vaccine production since it helps preserve chains A and B cross-linking in the process of the toxin to toxoid conversion, and it furthermore prevents presentation of hydrophobic amino acids on the surface that causes natural instability (Paliwal and London, 1996).

The final conformation of macromolecular ensembles can be predicted by the minimization of SASA when it applies to the interaction of protein surfaces (Richmond, 1984). To assess the DT structure hydrophobicity, the SASA of the residues was computed across each frame in an MD trajectory (Figure 4), indicating that hydrophobicity of DT conformation decreased at 27 ˚C and 37 ˚C in the selected simulation time scale. This result suggested that the conformational stability of the DT structure was reduced as a result of increasing its hydrophobicity at 47˚C. This finding was in line with the results of some experimental studies postulating that an increase

in temperature might cause alteration to the conformation, and therefore, might reflect the denaturation of DT (Pappenheimer Jr, 1937).

The corresponding percentages of secondary structure elements were analyzed using YASARA View program to get some more insights into the structural stability of DT at three different temperature levels (www.yasara.org). As indicated in Table 1, the highest β-sheets percentage of the DT structure was obtained at 37˚C, whereas the highest percentage of α-helix was observed at 27˚C.

In order to investigate the effect of temperature on the tertiary structure of DT, the contact maps were evaluated through CMView (version 1.1.1) (Vehlow et al., 2011). A contact map represents particularly a protein's 3D structure in a two-dimension form. The contact maps of DT were generated for chain A at three different temperatures (Figure 5). As it is obvious from Figure 5, the structures at 37˚C and 47˚C are different in the D68-K76, R173, G174, and A185-C186. However, the structures at 37˚C and 27˚C are similar in this regard. In addition, the disulfide bridge found in the region C186-C201 was conserved at 37˚C and 27˚C.

In the last section of this study, B-cell epitopes predicted by ElliPro for DT's conformations were obtained at three temperature levels (Table 2). The three sets of resulted B-cell epitope residues were also compared in this study. The DT structure at 47˚C had the conformational B-cell epitopes comprising of the largest number of amino acid residues. The majority of the amino acid residues forming the conformational B-cell epitopes of the DT structure at 37˚C resided in the catalytic domain. In addition, the conformational B-cell epitopes in the region including C186-C201 was only present at the DT structure at 37˚C.

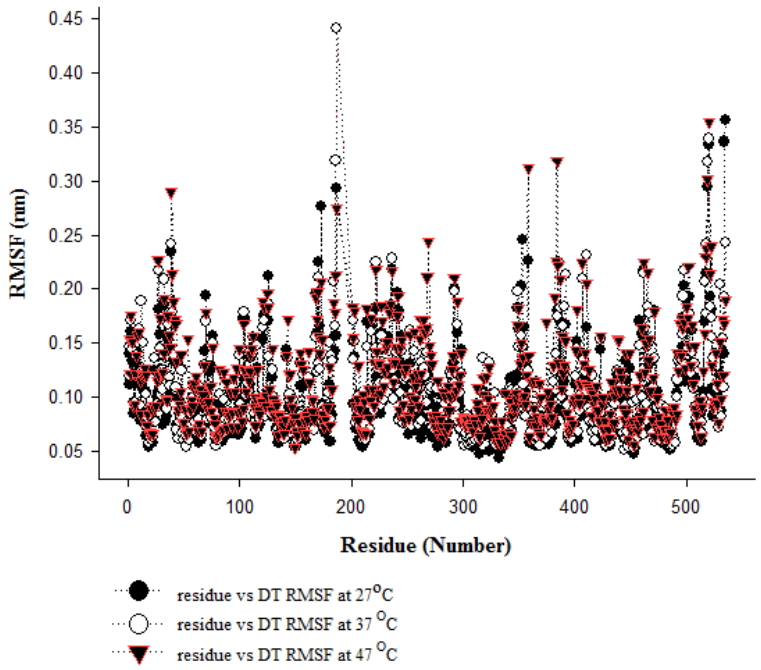

Figure 1. Comparison of the RMSF of the DT structures after 20ns timescale simulation at different temperature levels (27˚C, 37˚, and 47˚C). Symbols (-•-), (-o-), and (-▼-) correspond to RMSF of DT at 27˚C, 37˚C, and 47˚, respectively.

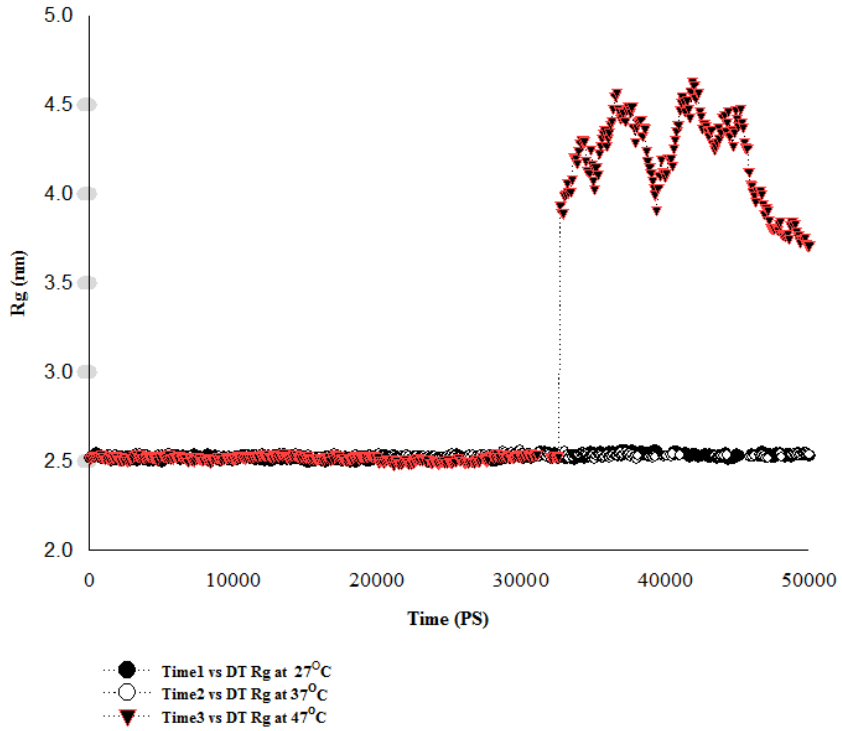

Figure 2. Comparison of the Rg of the DT structures after 20ns timescale simulation at different temperature levels (27˚C, 37˚C, and 47˚C). Symbols (-•-), (-o-), and (-▼-) correspond to the Rg of DT at 27˚C, 37˚C, and 47˚C, respectively.

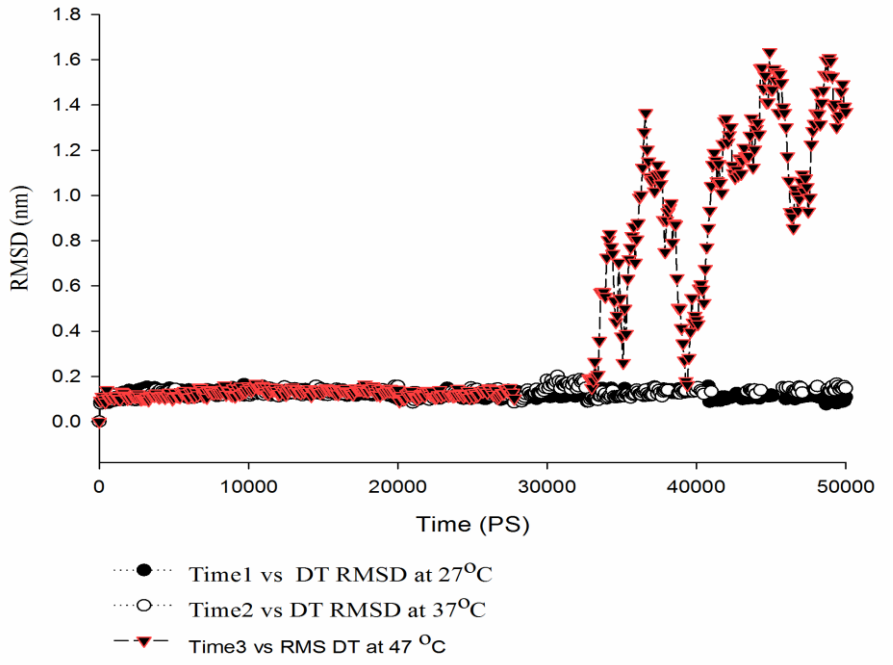

Figure 3. Comparison of the RMSD of the DT structures after 20ns timescale simulation at different temperature levels (27˚C, 37˚C, and 47˚C). Symbols (-•-), (-o), and (-▼-) correspond to the RMSD of DT at 27˚C, 37˚, and 47˚, respectively.

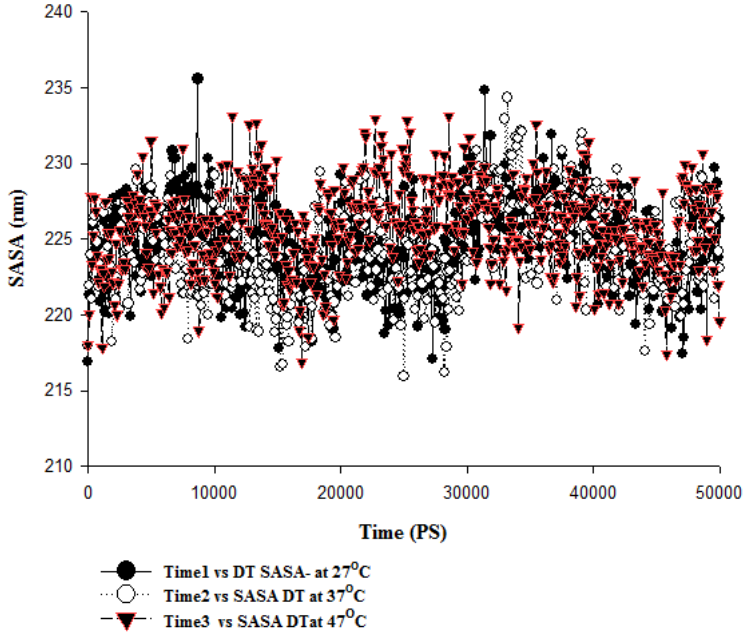

Figure 4. Diagram comparing the solvent-accessible surface area (SASA) of the residues in DT structure across each frame in an MD trajectory in different temperature levels (27˚C, 37˚C, and 47˚C). Symbols (-•-), (-o-), and (-▼-) correspond to the SASA of DT at 27˚C, 37˚C, and 47˚C, respectively;

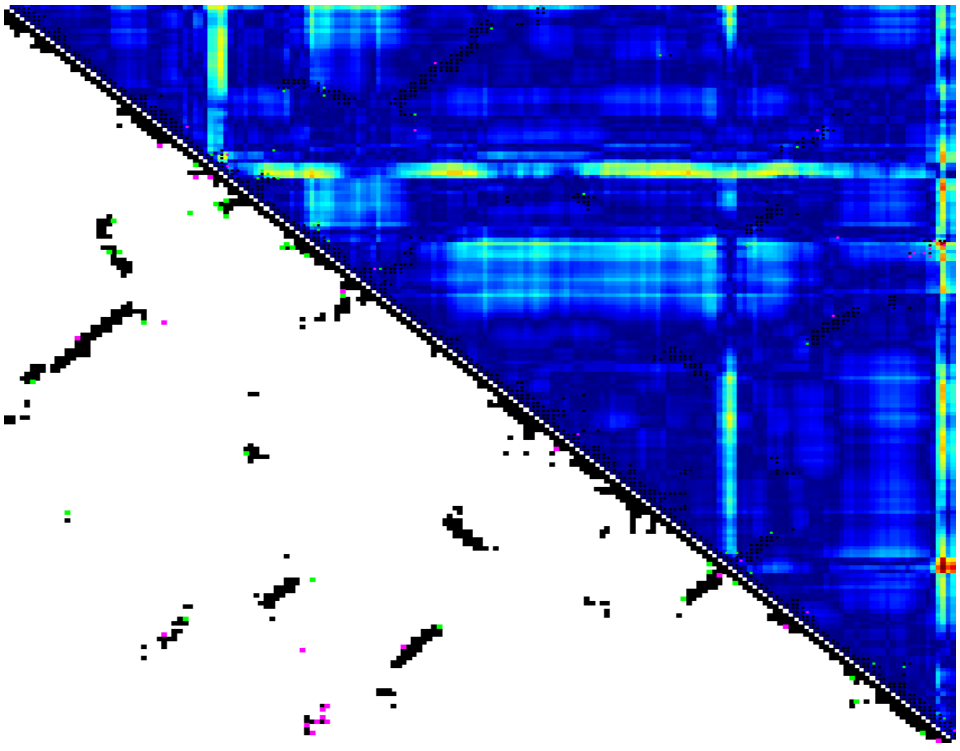

Figure 5A

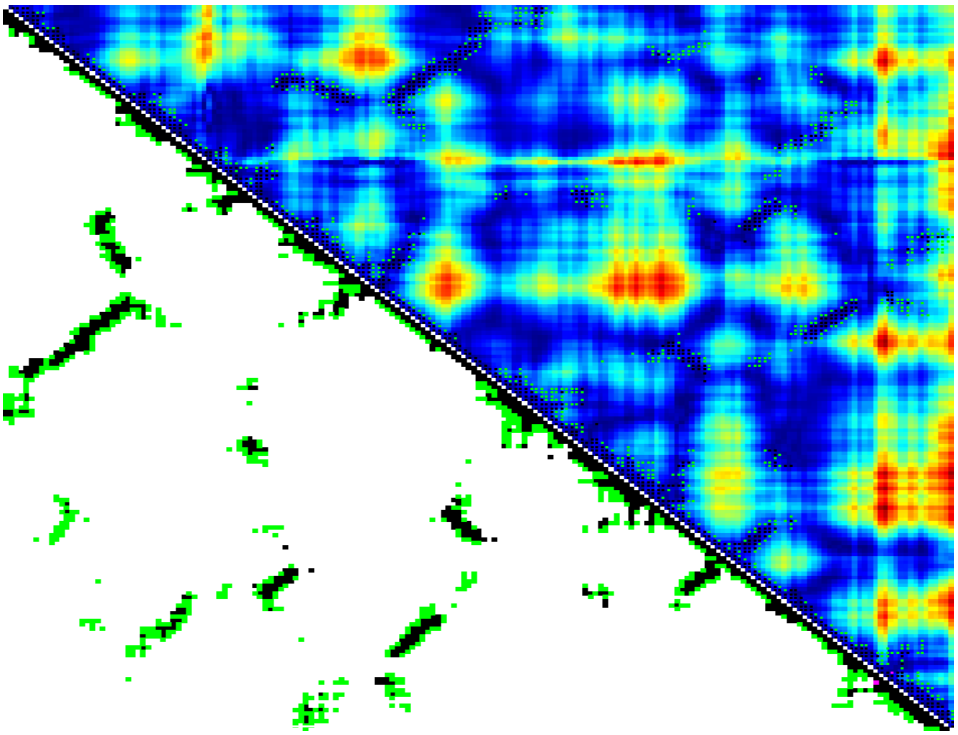

Figure 5B

Figure 5. A) Comparison of the contact map of chain A of the DT at 27˚C and 37˚C. **B)** Comparison of the contact map of chain A of the DT at 27˚C and 47˚C. Black points display the common contacts. Pink dots showing the contacts at 27˚C, which do not exist at 37˚C or 47˚C. Green dots demonstrating the contacts at 27˚C or 37˚C not existing at 47˚C.

Table 1. Comparison of the DT secondary structure at different temperature levels (27˚C, 37˚C, and 47˚C) after 50 ns simulation in the water

Secondary Structure %	27˚C	37˚C	47˚C
Helix	27.3	22.1	23.3
Sheet	26.3	27. 3	25.4
Turn	13.7	15.8	16.8
Coil	29.4	31.5	34.6

Table 2. Proprietary amino acids of the B-cell epitopes distinguished at different temperature levels.

B-cell epitopes at domain C of DT (27°C)	**B-cell epitopes at domain C of DT (37°C)**	**B-cell epitopes at domain C of DT (47°C)**
N45, A:Y46, A:D47, A:D48, A:D49, A:W50, A:K51, A:V91, A:L92, A:A93, A:V96, A:D97, A:N98, A:A99, A:E100, A:T101, A:I102, A:K103, A:S109, A:L110, A:T111, A:E112, A:P113, A:L114, A:M115, A:E116, A:Q117, A:V118, A:G119, , A:E122, A:F123, A:V134, A:N152, A:E154, A:Q155, A:K157	A:R173, A:C186, A:A187, B:C201, B:N203, B:L204, B:D205, B:W206, B:D207, B:V208, B:I209, B:R210, A:S18, A:G26, A:V28, A:D29, A:S30, A:Q32, A:K33, A:G34, A:K59, A:G78, A:K82, A:T84, A:A158, A:L159, A:S160, A:V161, A:E162, A:L163, A:E164, A:I165, A:N166, A:E168, A:T169, A:R170	A:S18, A:P25, A:G26, A:Y27, A:V28, A:D29, A:S30, A:I31, A:Q32, A:K33, A:G34, A:I35, A:Q36, A:K59, A:G78, A:V81, A:K82, A:V83, A:T84, A:A156, A:A158, A:L159, A:S160, A:V161, A:E162, A:L163, A:E164, A:I165, A:N166, A:F167, A:E168, A:T169, A:R170, A:G171, A:K172, B:C201, A:K37, A:P38, A:K39, A:S40, A:G41, A:T42, A:Q43,

Discussion

With an emphasis on investigating the effect of temperature on B-cell epitopes, this study was performed to evaluate the conformational changes of the DT structure at different temperatures, including (27˚C, 37˚C, and 47˚C) using MD simulations. Significant decreases were observed in percentages of β-sheets, turns, and helices of the DT structure at 47˚C in comparison with those at 27˚C and 37˚C. The results also showed that the RMSD of the DT structure increased upon increasing the temperature to more than 37˚C. The amino acid fluctuations were similar at 27˚C and 37˚C in the C and R domains. However, at the junction of chains A and B (C186-C201) and 37˚C, they were higher than those at 27˚C. Furthermore, the amino acid fluctuations in the T domain at 47˚C were much higher than those in the C and R domains. Our findings demonstrated that the stability of the DT structure decreased at 47˚C as a result of increasing Rg as well as RMSD. The overall view of the results suggested that DT's conformational changes at 27˚C and 37˚C are comparable whereas these changes are dramatic at 47 ˚C. It does seem as though the temperature level around 47 ˚C is a threshold for dramatic conformational changes of DT structure. This finding is completely in line with the results of some researchers (Lobanov et al., 2008). The results of the SASA diagram showed that the hydrophobicity of the DT structure increased upon the temperature rising. It was also found that the number of B-cell epitope residues increased by the rise in temperature level. However, B-cell epitopes belonging to the junction region of chains A and B were only present at 37˚C. Our results together demonstrated that some critical conformational B-cell epitopes of DT were preserved and would be introduced to the immune system at just 37˚C.This finding is in agreement with the applied temperature condition for the industrial production process of DT vaccines. Therefore, the method used in this study can be applied to determine appropriate temperature conditions for the protein-based vaccine production. Accordingly, it is expected to be useful for the production of novel vaccines and improvement of current vaccines.

Authors' Contribution

Study concept and design: S. Gh. and M.R. B.
Acquisition of data: S. Gh.
Analysis and interpretation of data: S. Gh. and M. A.
Drafting of the manuscript: M. A.
Critical revision of the manuscript for important intellectual content: M. A., S. Gh. and Sh. T.
Statistical analysis: M. A.
Administrative, technical, and material support: S. Gh., M. A. and Sh. T.

Ethics

We hereby declare all ethical standards have been met in the preparation of this article.

Conflict of Interest

We declare no conflict of interest.

Grant Support

This study was supported by RVSRI, Agricultural Research, Education, and Extension Organization.

Acknowledgment

The authors wish to thank Dr. Movahedi, A.R. for consultation during this study.

References

Abraham, M.J., Murtola, T., Schulz, R., Páll, S., Smith, J.C., Hess, B., *et al.*, 2015. GROMACS: High performance molecular simulations through multi-level parallelism from laptops to supercomputers. SoftwareX 1, 19-25.

Anandakrishnan, R., Aguilar, B., Onufriev, A.V., 2012. H++ 3.0: automating p K prediction and the preparation of biomolecular structures for atomistic molecular modeling and simulations. Nucleic Acids Res 40, 537-541.

Arfken, G., 1985. The method of steepest descents. Math Methods Phys 3, 428-436.

Audibert, F., Jolivet, M., Chedid, L., Alouf, J., Boquet, P., Rivaille, P., *et al.*, 1981. Active antitoxic immunization by a diphtheria toxin synthetic oligopeptide. Nature 289, 593-594.

Boquet, P., Alouf, J.E., Duflot, E., Siffert, O., Rivaille, P., 1982. Characteristics of guinea-pig immune sera elicited by a synthetic diphtheria toxin oligopeptide. Mol Immunol 19, 1541-1549.

Brüschweiler, R., 2003. Efficient RMSD measures for the comparison of two molecular ensembles. Proteins 50, 26-34.

Bussi, G., Donadio, D., Parrinello, M., 2007. Canonical sampling through velocity rescaling. J Chem Phys 126, 014101.

Chenal, A., Nizard, P., Gillet, D., 2002. Structure and function of diphtheria toxin: from pathology to engineering. J Toxicol: Toxin Rev 21, 321-359.

Darden, T., York, D., Pedersen, L., 1993. Particle mesh Ewald: An N· log (N) method for Ewald sums in large systems. J Chem Phys 98, 10089-10092.

Diamond, R., 1976. On the comparison of conformations using linear and quadratic transformations. ACTA Crystall A-CRYS 32, 1-10.

Diamond, R., 1988. A note on the rotational superposition problem. Acta Crystallogr A: Found Crystallogr 44, 211-216.

Falnes, P.O., Olsnes, S., 1995. Cell-mediated reduction and incomplete membrane translocation of diphtheria toxin mutants with internal disulfides in the A fragment. J Biol Chem 270, 20787-20793.

Ghaderi, S., Tarahomjoo, S., Bozorgmehr, M.R., 2016. Utilizing molecular dynamics simulations for identification of conformational B-cell epitopes in diphtheria toxin at varying pHs. J Chem, Biol Phys Sci 7, 85-91.

Gordon, V.M., Leppla, S.H., 1994. Proteolytic activation of bacterial toxins: role of bacterial and host cell proteases. Infect Immun 62, 333-340.

Grubmüller, H., Heller, H., Windemuth, A., Schulten, K., 1991. Generalized Verlet algorithm for efficient molecular dynamics simulations with long-range interactions. Mol Simulat 6, 121-142.

Guerineau, F., Sorensen, A.M., Fenby, N., Scott, R.J., 2003. Temperature sensitive diphtheria toxin confers conditional male- sterility in Arabidopsis thaliana. Plant Biotechnol J 1, 33-42.

Hess, B., Bekker, H., Berendsen, H.J., Fraaije, J.G., 1997. LINCS: a linear constraint solver for molecular simulations. J Comput Chem 18, 1463-1472.

Hornak, V., Abel, R., Okur, A., Strockbine, B., Roitberg, A., Simmerling, C., 2006. Comparison of multiple Amber force fields and development of improved protein backbone parameters. Proteins 65, 712-725.

Johnson, A., Johnson, T., Khan, A., 2012. Thermostats in Molecular Dynamics Simulations. UMass 1, 29.

Jorgensen, W.L., Chandrasekhar, J., Madura, J.D., Impey, R.W., Klein, M.L., 1983. Comparison of simple potential functions for simulating liquid water. J Chem Phys 79, 926-935.

Kabsch, W., 1976. A solution for the best rotation to relate two sets of vectors. ACTA Crystall A-CRYS 32, 922-923.

Kabsch, W., Sander, C., 1983. Dictionary of protein secondary structure: pattern recognition of hydrogen-bonded and geometrical features. Biopolymers 22, 2577-2637.

Kövér, K., Bruix, M., Santoro, J., Batta, G., Laurents, D., Rico, M., 2008. The solution structure and dynamics of human pancreatic ribonuclease determined by NMR spectroscopy provide insight into its remarkable biological activities and inhibition. J Mol Biol 379, 953-965.

Kräutler, V., Van Gunsteren, W.F., Hünenberger, P.H., 2001. A fast SHAKE algorithm to solve distance constraint equations for small molecules in molecular dynamics simulations. J Comput Chem 22, 501-508.

Krieger, E., Vriend, G., 2015. New ways to boost molecular dynamics simulations. J Comput Chem 36, 996-1007.

Laurents, D., Pérez- Cañadillas, J.M., Santoro, J., Rico, M., Schell, D., Pace, C.N., *et al.*, 2001. Solution structure and dynamics of ribonuclease Sa. Proteins 44, 200-211.

Lobanov, M.Y., Bogatyreva, N., Galzitskaya, O., 2008. Radius of gyration as an indicator of protein structure compactness. Mol Biol 42, 623-628.

London, E., 1992. Diphtheria toxin: membrane interaction and membrane translocation. Biochim Biophys Acta 1113, 25-51.

Menestrina, G., Schiavo, G., Montecucco, C., 1994. Molecular mechanisms of action of bacterial protein toxins. Mol Aspects Med 15, 79-193.

Oh, K.J., Zhan, H., Cui, C., Hideg, K., Collier, R.J., Hubbell, W.L., 1996. Organization of diphtheria toxin T domain in bilayers: a site-directed spin labeling study. Science 273, 810-812.

Paliwal, R., London, E., 1996. Comparison of the conformation, hydrophobicity, and model membrane interactions of diphtheria toxin to those of formaldehyde-treated toxin (diphtheria toxoid): formaldehyde stabilization of the native conformation inhibits changes

that allow membrane insertion. Biochemistry 35, 2374-2379.

Pappenheimer Jr, A., 1937. Diphtheria Toxin. I. Isolation and Characterization of a Toxic Protein from Corynebacterium diphtheriae Filtrates. J Biol Chem 120, 543-553.

Parrinello, M., Rahman, A., Vashishta, P., 1983. Structural transitions in superionic conductors. Phys Rev Lett 50, 1073-1076.

Purohit, R., Rajendran, V., Sethumadhavan, R., 2011. Relationship between mutation of serine residue at 315th position in M. tuberculosis catalase-peroxidase enzyme and Isoniazid susceptibility: an in silico analysis. J Mol Model 17, 869-877.

Purohit, R., Sethumadhavan, R., 2009. Structural basis for the resilience of Darunavir (TMC114) resistance major flap mutations of HIV-1 protease. Interdiscip Sci 1, 320-328.

Rajendran, V., Purohit, R., Sethumadhavan, R., 2012. In silico investigation of molecular mechanism of laminopathy caused by a point mutation (R482W) in lamin A/C protein. Amino Acids 43, 603-615.

Richmond, T.J., 1984. Solvent accessible surface area and excluded volume in proteins: Analytical equations for overlapping spheres and implications for the hydrophobic effect. J Mol Biol 178, 63-89.

Salomon- Ferrer, R., Case, D.A., Walker, R.C., 2013. An overview of the Amber biomolecular simulation package. Wiley Interdiscip Rev Computa Mol Sci 3, 198-210.

Satpathy, R., Guru, R.K., Behera, R., Priyadarshini, A., 2010. Homology modelling of lycopene cleavage oxygenase: The key enzyme of bixin production. J Comput Sci Syst Biol 3, 059-061.

Steere, B., Eisenberg, D., 2000. Characterization of high-order diphtheria toxin oligomers. Biochemistry 39, 15901-15909.

Vehlow, C., Stehr, H., Winkelmann, M., Duarte, J.M., Petzold, L., Dinse, J., *et al.*, 2011. CMView: interactive contact map visualization and analysis. Bioinformatics 27, 1573-1574.

Vendome, J., Posy, S., Jin, X., Bahna, F., Ahlsen, G., Shapiro, L., *et al.*, 2011. Molecular design principles underlying β-strand swapping in the adhesive dimerization of cadherins. Nat Struct Mol Biol 18, 693-700.

Zhao, J.-M., London, E., 1986. Similarity of the conformation of diphtheria toxin at high temperature to that in the membrane-penetrating low-pH state. P Natl A Sci 83, 2002-2006.

Zhao, Y., Zeng, C., Massiah, M.A., 2015. Molecular Dynamics Simulation Reveals Insights into the Mechanism of Unfolding by the A130T/V Mutations within the MID1 Zinc-Binding Bbox1 Domain. PloS one 10, e0124377.

Zhou, Z., Feng, H., Ghirlando, R., Bai, Y., 2008. The high-resolution NMR structure of the early folding intermediate of the Thermus thermophilus ribonuclease H. J Mol Biol 384, 531-539.